

## Membrane Channel-forming Polypeptides

### AQUEOUS PHASE AGGREGATION AND MEMBRANE-MODIFYING ACTIVITY OF SYNTHETIC FLUORESCENT ALAMETHICIN FRAGMENTS\*

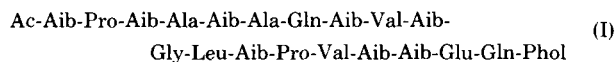
(Received for publication, June 12, 1981)

Mathew K. Mathew‡, Ramakrishnan Nagaraj, and Padmanabhan Balaram§

From the Molecular Biophysics Unit, Indian Institute of Science, Bangalore-560 012, India

Synthetic fragments of the membrane channel-forming polypeptide, alamethicin, have been labeled with a fluorescent 5-dimethylaminonaphthalene-1-sulfonyl (dansyl) group at the NH<sub>2</sub>-terminal. Seventeen and 13-residue fluorescent peptide esters have been shown to translocate divalent cations in unilamellar liposomes and uncouple oxidative phosphorylation in rat liver mitochondria. The corresponding peptide acids also exhibit membrane-modifying activity, whereas the shorter fragments are inactive. Aggregation of fluorescent peptides in aqueous solutions leads to a marked blue shift and enhancement of the dansyl group emission spectrum. "Critical micelle" concentrations may be determined for the association of peptides. The longer peptides aggregate at lower concentrations than the short peptides, with the ease of aggregation following a trend similar to that for functional activity. The peptide acids aggregate only in media of high ionic strength. The peptide ester aggregates are stabilized by increasing salt concentration and dissociated by urea, suggestive of hydrophobic stabilization of the aggregates. The enthalpy of association for the 10- and 17-residue peptide esters is estimated to be between -1 and -3 kcal mol<sup>-1</sup> of monomer. The aqueous phase aggregation of channel-forming peptides at low concentrations suggests that preformed aggregates may be inserted into the membrane to constitute functional channels.

Alamethicin (I), a 20-residue polypeptide antibiotic produced by *Trichoderma viride*, has been extensively studied because of its membrane-modifying properties (1, 2).



The polypeptide is rich in the unusual amino acid,  $\alpha$ -aminoisobutyric acid (Aib)<sup>1</sup>, a residue which considerably restricts

\* This study was supported by a grant from the Department of Science and Technology, Government of India. The costs of publication of this article were defrayed in part by the payment of page charges. This article must therefore be hereby marked "advertisement" in accordance with 18 U.S.C. Section 1734 solely to indicate this fact.

‡ Recipient of a fellowship from the Indian Council of Medical Research.

§ Recipient of a University Grants Commission Career Award.

<sup>1</sup> The abbreviations used are: Aib,  $\alpha$ -aminoisobutyric acid; dansyl, 5-dimethylamino naphthalene-1-sulfonyl; D-(1-*n*)-OBz, *N*-dansylglycyl peptide benzyl ester of the peptide consisting of the first *n* residues in I; D-(1-*n*)-OH, *N*-dansylglycyl peptide acid of the peptide consisting of the first *n* residues in I; HEPES, 4-(2-hydroxyethyl)-1-piperazine ethanesulfonic acid; Tris, tris(hydroxymethyl)methylamine; cmc, crit-

ical micelle concentration; Z, benzyloxycarbonyl; EPC, egg phosphatidylcholine.

the conformational flexibility of the peptide backbone (3). Closely related Aib-containing polypeptides like suzukacillin (4, 5) and trichotoxin A-40 (6) have been shown to similarly modify membrane conductance, probably by the formation of transmembrane channels (5, 6). Although most studies on alamethicin have used model lipid membrane systems, the polypeptide has been reported to increase calcium permeability of sarcoplasmic reticulum vesicles (7), uncover latent adenylate cyclase activity (8), and lyse erythrocytes (9) and leukocytes (10). It also causes fusion of lipid vesicles (11) and has been used to assay sidedness of natural membrane systems (8).

Conformational studies of model Aib-containing peptides (12-16) and synthetic fragments of alamethicin (17-20) and suzukacillin (21, 22) reveal that these polypeptides are likely to adopt highly folded 3<sub>10</sub> helical conformations, in which the helix interior is too narrow to permit passage of cations. The functional channel may be composed of an aggregate of these rigid, hydrophobic, helical polypeptides. Such a structure would contain a central aqueous core, which would span the lipid bilayer. Studies of the electrical properties of alamethicin-modified bilayer lipid membranes confirm that the functional channel does contain an aggregate of alamethicin monomers (23). Estimates of the aggregation number have been varied, with pentamers or hexamers being favored for the higher conductance states (23-25). The site of aggregation of the monomer units has not yet been firmly established. Both aqueous phase (23) and membrane phase (26) aggregation have been proposed, with the aggregate in the former case inserting into the lipid membrane in response to an electric field (23).

We have earlier reported on the effects of chain length and charge of synthetic alamethicin fragments on the divalent cation permeability of unilamellar liposomes (27) and on uncoupling of oxidative phosphorylation in rat liver mitochondria (28). In order to study peptide aggregation at low concentrations, we have synthesized fluorescent peptide derivatives of alamethicin fragments. Emission parameters of the dansyl fluorophore have been shown to be sensitive to peptide aggregation (29). In this report, we show that the membrane activities of *N*-dansylglycyl alamethicin fragments, as measured by their ability to translocate cations in liposomes and their uncoupling of oxidative phosphorylation in mitochondria, parallel those of the parent peptide. We further examine the aqueous phase aggregation behavior of the synthetic, fluorescent alamethicin fragments to establish the effect of chain length, charge, and ionic strength on peptide association and attempt to correlate membrane-modifying activity with ease of aggregation.

ical micelle concentration; Z, benzyloxycarbonyl; EPC, egg phosphatidylcholine.

## THEORY

The aqueous phase aggregation behavior of hydrophobic peptides is analogous to micellar association of amphipathic molecules like detergents and phospholipids (30). It is convenient to analyze the results obtained in terms of models used in studies of micellar aggregation.

Tanford (31) has estimated the change in chemical potential on micellization to be

$$\mu_{\text{mic}}^{\circ} - \mu_{\text{w}}^{\circ} = \frac{\bar{m} - 1}{\bar{m}} RT \ln \text{cmc} + RT \ln f_{\text{w}} + \frac{RT}{\bar{m}} \ln (\sigma \bar{m}) \quad (1)$$

where the subscripts mic and W refer to micellar and aqueous phases, respectively.  $\bar{m}$  is the average aggregation number,  $f_{\text{w}}$  is the activity coefficient of the hydrated monomer, and  $\sigma$  is a constant that lies between 1 and 100.

In the case of alamethicin fragments, the cmc values have been found to be in the micromolar range (see "Results"), where  $f_{\text{w}}$  will be  $\sim 1$ . Since  $\Delta G = \mu_{\text{mic}}^{\circ} - \mu_{\text{w}}^{\circ}$ , Equation 1 may be rewritten as

$$\Delta G = \frac{\bar{m} - 1}{\bar{m}} RT \ln \text{cmc} + \frac{RT}{\bar{m}} \ln (\sigma \bar{m}) \quad (2)$$

The enthalpy change  $\Delta H$  is given by

$$\Delta H = \frac{d \Delta G / T}{d 1/T} = \frac{\bar{m} - 1}{\bar{m}} R \cdot \frac{d \ln \text{cmc}}{d 1/T} + \frac{R d [\ln (\sigma \bar{m})] / \bar{m}}{1/T} + R \ln \text{cmc} \frac{d \frac{\bar{m} - 1}{\bar{m}}}{d 1/T} + \frac{R d \ln \sigma}{\bar{m} d 1/T} \quad (3)$$

$\sigma$  is a constant and  $\bar{m}$  is not likely to be sensitive to temperature. Hence,

$$\Delta H = \frac{\bar{m} - 1}{\bar{m}} R \frac{d \ln \text{cmc}}{d 1/T} \quad (4)$$

Determination of the temperature dependence of cmc values can, therefore, yield  $\Delta H$ . A plot of  $\ln \text{cmc}$  versus  $1/T$  should be linear if the dependence of  $\Delta H$  on temperature is small, i.e. the heat capacity of the system is low. The slope gives  $(\bar{m}/\bar{m} - 1) \Delta H$ .

## MATERIALS AND METHODS

All peptides were synthesized by solution phase procedures. Illustrative procedures have been described for alamethicin fragments (32). Boc-Gly was used at the  $\text{NH}_2$  terminus to facilitate dansylation of the amino group. Fluorescent peptides were purified by column chromatography on silica gel. The peptides were shown to be homogeneous by thin layer chromatography and were characterized by 270 MHz  $^1\text{H}$  NMR. The peptides used in this study are abbreviated as D-(1- $n$ )-OBz where D refers to the *N*-dansylglycyl group and OBz to the benzyl ester function, and  $n$  is the residue number in the alamethicin sequence (I). The corresponding carboxylic acids are denoted as D-(1- $n$ )-OH. Egg phosphatidylcholine, Sephadex G-50 (coarse), chlortetracycline, X537 A, HEPES, Tris, and ADP were from Sigma Chemical Co. All other chemicals were of analytical grade. Fluorescence measurements were made on a Perkin-Elmer MPF-44A fluorescence spectrometer operated in the ratio mode with 5-nm excitation and emission band pass unless otherwise mentioned.

**Cation Transport in Liposomes**—Small unilamellar vesicles were generated by the removal of cholate from mixed micelles of EPC and cholate by gel filtration on Sephadex G-50 (33). Ion translocation was followed using  $25 \mu\text{M}$  chlortetracycline and  $200 \mu\text{g/ml}$  of EPC vesicles in  $5 \text{ mM}$  HEPES and  $100 \text{ mM}$  NaCl (pH 7.0). After CTC had equilibrated across the membrane,  $\text{Ca}^{2+}$  was added at  $1 \text{ mM}$ , following which ionophore was introduced. The fluorescence of the chlortetracycline- $\text{Ca}^{2+}$  complex was monitored with 10-nm excitation and emission band pass;  $\lambda_{\text{ex}} = 390 \text{ nm}$ ,  $\lambda_{\text{em}} = 530 \text{ nm}$ . One-cm square cells were used and solutions stirred with a magnetic pellet to minimize settling. Vesicle integrity was checked by a step response after adding metal ions, followed by a sharp rise on adding  $20 \mu\text{M}$  X537 A (27).

**Uncoupling of Oxidative Phosphorylation**—Mitochondria were

isolated from the livers of adult, male rats by the method described (34). Respiratory rates of the mitochondria were measured on a Gilson model K-ICT-C oxygraph fitted with a Clark oxygen electrode at  $30^\circ\text{C}$  in a medium containing  $53 \text{ mM}$  sucrose,  $2.1 \text{ mM}$  EDTA,  $7.1 \text{ mM}$   $\text{MgCl}_2$ ,  $110 \text{ mM}$  Tris-HCl, and  $21 \text{ mM}$  potassium phosphate, pH 7.4, in a total volume of 1.4 ml. Succinate ( $18 \text{ mM}$ ) was used as substrate. Peptide in ethanol was added to state 4 mitochondria, such that no more than  $5 \mu\text{l}$  of solution were added. Five  $\mu\text{l}$  of ethanol had no detectable effect on the respiration of mitochondria. Due to the hydrophobicity of the peptides, the cell had to be rinsed with mitochondria between experiments to remove the last traces of uncoupler (28). Protein was estimated by the biuret method (35).

**Aggregation-Disaggregation Studies**—Dansylated peptides in methanol were added to aqueous solutions at various concentrations and emission spectra recorded, with  $\lambda_{\text{ex}} = 333 \text{ nm}$ . A period of 5 min was allowed to elapse between measurements following each addition. The alcohol concentration was kept below 1%. The dilution arms of the curve were generated by sequential dilution from the highest concentration used in the aggregation titration. The time course of the disaggregation process was followed by rapidly diluting aggregated peptide solutions to double their volume and recording spectra at intervals of time. Variable temperature studies were carried out using a thermostatted cell assembly. Temperature was maintained constant

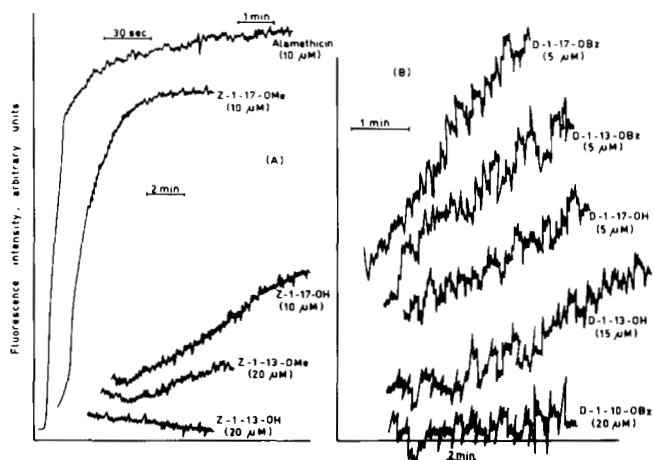


FIG. 1. Cation-translocating activity of alamethicin fragments. Time-dependent increases in chlortetracycline- $\text{Ca}^{2+}$  fluorescence in response to the addition of peptides. Peptides were added just prior to the start of the recording. Peptides and concentrations used are marked in figure. Time scales: (A) top time scale for alamethicin, lower time scale for all other peptides; (B) lower time scale for D-1-10-OBz, upper time scale for all other peptides. Note that the traces in B have been recorded at a higher sensitivity than those in A. Time  $t = 0$  is at the start of the trace.

TABLE I

## Comparison of membrane-modifying activity with ease of aggregation of fluorescent alamethicin fragments

Cation-translocating ability assayed by liposome technique and expressed as initial slope for  $5 \mu\text{M}$  peptide. Uncoupling activity expressed as per cent reduction in RCI by  $2.8 \mu\text{M}$  peptide. Ease of aggregation expressed as critical micelle concentration. All procedures described under "Materials and Methods."

| Peptide    | Liposome transport (initial slope for $5 \mu\text{M}$ peptide) | Uncoupling activity (% reduction in RCI by $2.8 \mu\text{M}$ peptide) | Ease of aggregation (cmc) |
|------------|--|---|---------------------------|
| D-1-17-OBz | 1.9  | 90  | $10 \mu\text{M}$          |
| D-1-17-OH  | 0.5  | 44  | $>50$                     |
| D-1-13-OBz | 0.7  | 90  | 3                         |
| D-1-13-OH  | $0.6^a$  | 30  | $>50$                     |
| D-1-10-OBz | $0^b$  | $0^b$   | 30                        |
| D-1-6-OBz  | $0^b$  | $0^b$   | $>50$                     |

<sup>a</sup> At  $15 \mu\text{M}$ .

<sup>b</sup> At  $20 \mu\text{M}$ .

to  $\pm 0.1$  °C. Five min were allowed to elapse following attainment of a steady temperature before spectra were recorded.

### RESULTS

**Ca<sup>2+</sup> Translocation in Liposomes**—Ca<sup>2+</sup> influx into chlortetracycline-containing liposomes results in the formation of highly fluorescent chlortetracycline-Ca<sup>2+</sup> complexes (27, 36). A rise in fluorescence emission with time after addition of ionophore may, therefore, be used to monitor the ion-translocating ability of the peptides, as shown earlier (27). Fig. 1 compares the time dependences of the increase in fluorescence of chlortetracycline entrapped in liposomes following addition of dansylated and parent peptides. A convenient parameter for quantitatively assessing the activities of different peptides

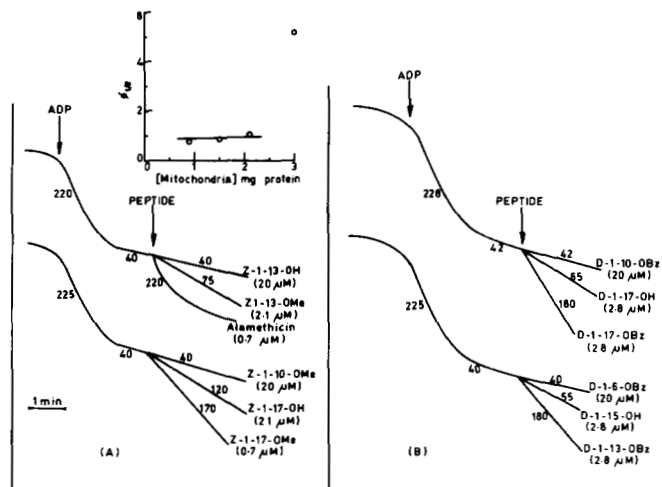


FIG. 2. Uncoupling of mitochondrial oxidative phosphorylation. Conditions as under "Materials and Methods." Peptides and concentrations used are indicated in the figure. Numbers against the traces indicate oxygen uptake in nanoatoms of  $O \cdot \text{min}^{-1}$  ( $\text{mg}$  of protein)<sup>-1</sup>. Inset, variation of  $\phi_{1/2}$  for Z-1-17-OMe with mitochondrial concentration.

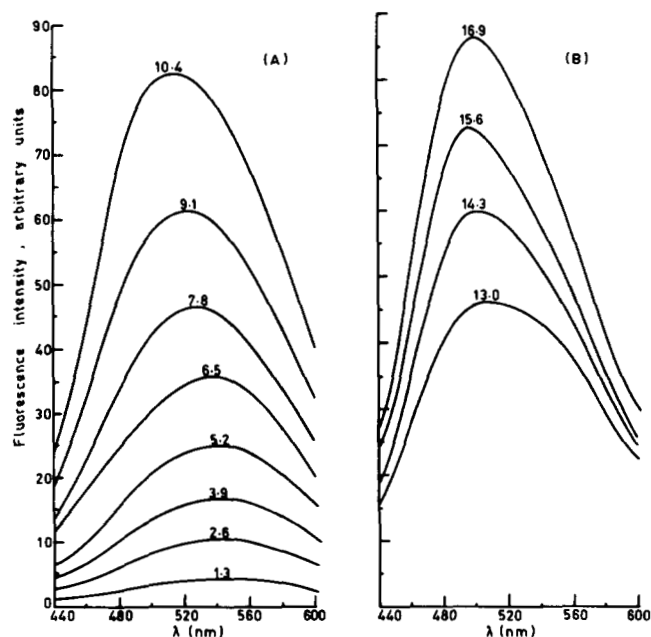


FIG. 3. Emission spectra of D-1-17-OBz excited at 333 nm as a function of peptide concentration. Peptide concentration ( $\mu\text{M}$ ) indicated against the traces. Concentrations 13  $\mu\text{M}$  and above recorded at 0.3 times the sensitivity used for the lower concentrations.

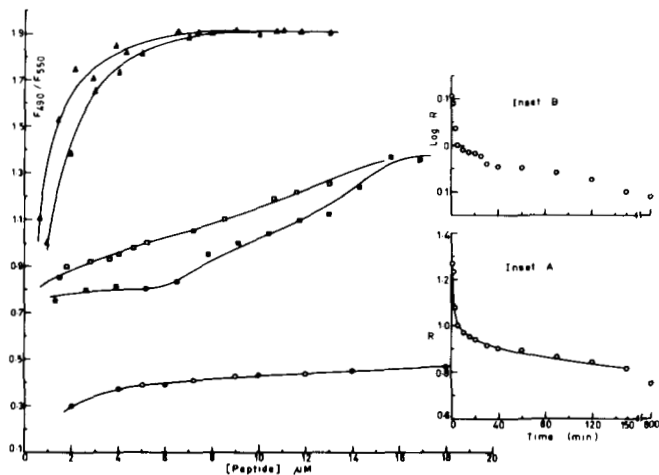


FIG. 4. Aggregation of fluorescent alamethicin fragments D-1-13-OBz ( $\Delta$ - $\Delta$ ), D-1-17-OBz ( $\square$ - $\square$ ), and D-1-17-OH ( $\circ$ - $\circ$ ). Filled symbols represent aggregation, open symbols sequential dilution. Conditions as given under "Materials and Methods."  $R = F_{490}/F_{550}$ . Insets, rate of change of  $R$  following rapid dilution of aggregated D-1-17-OBz from 20  $\mu\text{M}$  to 10  $\mu\text{M}$ . A,  $R$  versus time; B,  $\log R$  versus time.

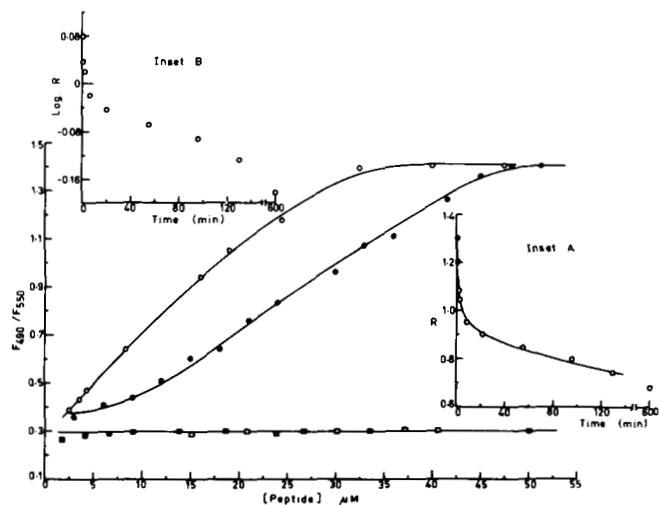


FIG. 5. Aggregation of fluorescent alamethicin fragments.  $\circ$ - $\circ$ , D-1-10-OBz;  $\square$ - $\square$ , D-1-6-OBz. Filled symbols represent aggregation, open symbols sequential dilution.  $R = F_{490}/F_{550}$ . Insets, rate of change of  $R$  following rapid dilution of aggregated D-1-10-OBz from 52  $\mu\text{M}$  to 26  $\mu\text{M}$ . A,  $R$  versus time; B,  $\log R$  versus time. All conditions as given under "Materials and Methods."

is the initial slope of the fluorescence increase, immediately following peptide addition. Values of the initial slopes for the fluorescent fragments are presented in Table I. The activities of the *N*-dansylglycyl peptides compare well with those of the benzyloxycarbonyl-protected parent peptides. The sequence of ionophore activity for the dansylated peptides is D-1-17-OBz > D-1-13-OBz  $\sim$  D-1-17-OH > D-1-13-OH. D-1-10-OBz and smaller fragments are inactive. A similar activity sequence was determined for the nonfluorescent peptides (27).

**Uncoupling of Oxidative Phosphorylation**—Alamethicin (28, 37) and some of its synthetic fragments have been shown to uncouple oxidative phosphorylation in rat liver mitochondria (37). This property is probably a consequence of the formation of peptide channels, which serve to break down transmembrane gradients of cations, including protons (28). These peptides stimulate state 4 respiration in mitochondria in the absence of added ADP. Fig. 2 compares the uncoupling activity of some dansylated and parent peptides. Once again,

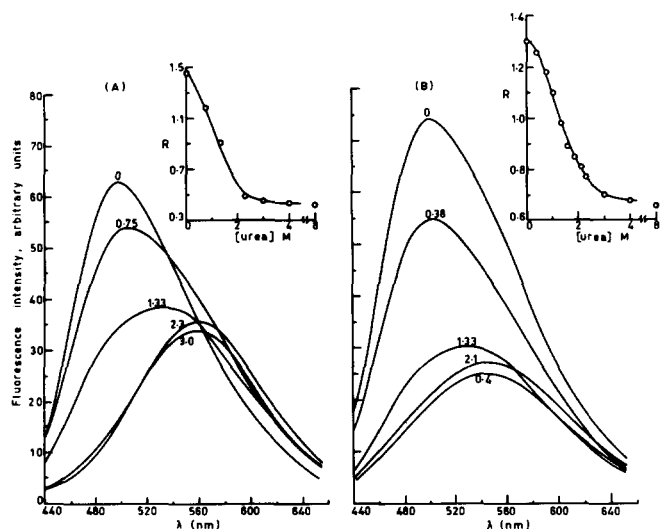


FIG. 6. Effect of urea on peptide aggregates. Emission spectra of fluorescent alamethicin derivatives, excited at 333 nm, as a function of urea concentration. Urea concentrations indicated against the traces. *Insets*, variations of  $R = F_{490}/F_{550}$  with urea concentration. A, 50  $\mu\text{M}$  D-1-10-OBz; B, 20  $\mu\text{M}$  D-1-17-OBz.

the activities of the labeled and parent peptides are comparable. The percentage reduction in the respiratory control index may be used to compare the activities of the various peptides. These values for the fluorescent fragments are summarized in Table I. The sequence of uncoupling activity for the dansylated peptides is D-1-17-OBz  $\sim$  D-1-13-OBz > D-1-17-OH > D-1-13-OH. D-1-10-OBz and smaller fragments are inactive. A similar sequence was obtained earlier for the parent peptides (28).

The *inset* to Fig. 2 shows the variation in  $\phi_{1/2}$  (concentration for half-maximal stimulation of state 4 respiration) for Z-1-17-OMe, with the concentration of mitochondria used. Up to 2 mg/ml of mitochondrial protein  $\phi_{1/2}$  is essentially independent of mitochondrial concentration. The similarities in the activity of parent and fluorescent peptides as monitored by the liposomal cation transport and uncoupling of oxidative phosphorylation assays suggest that introduction of the *N*-dansylglycyl group does not significantly affect the membrane-modifying properties of the peptides. The fluorescent fragments may, therefore, serve as useful models for further studies of peptide aggregation.

**Aggregation of Dansylated Peptides**—Fig. 3 shows emission spectra of D-1-17-OBz as a function of peptide concentration. At concentrations greater than 6  $\mu\text{M}$  D-1-17-OBz, the

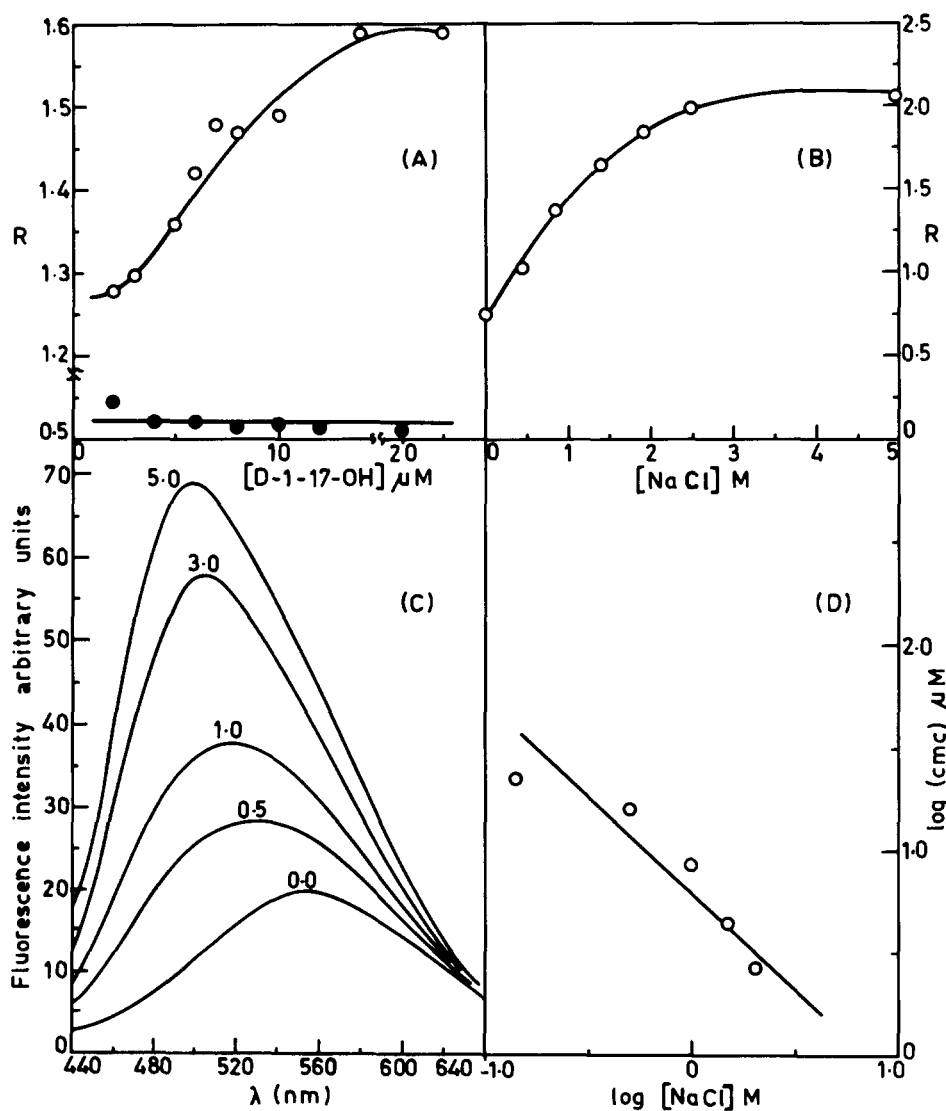


FIG. 7. Effect of NaCl on peptide aggregation. A, variation of  $R = F_{490}/F_{550}$  with concentration of D-1-17-OH in 3 M NaCl ( $\circ$ — $\circ$ ) or 1 M NaCl ( $\bullet$ — $\bullet$ ). B, variation of  $R$  with NaCl concentration for 9  $\mu\text{M}$  D-1-17-OBz. C, emission spectra of D-1-10-OBz (15  $\mu\text{M}$ ), excited at 333 nm, as a function of NaCl concentration. NaCl concentration (molar M) marked on the spectra. D, log-log plot of the variation of cmc of D-1-10-OBz as a function of NaCl concentration.

emission maximum shifts to lower wavelength with an enhancement in intensity. Peptide association can thus be easily monitored as in the case of emerimicin fragments (29). The ratio (R) of emission intensities at 490 nm to that at 550 nm ( $F_{490}/F_{550}$ ) is taken as an index of aggregation and plotted in Figs. 4 and 5 for all of the labeled peptides. The critical aggregation or critical micelle concentrations determined for the various peptides are listed in Table 1. The facility of aggregation follows the sequence D-1-13-OBz > D-1-17-OBz > D-1-10-OBz, while D-1-6-OBz and the acids did not aggregate in salt-free aqueous media.

Sequential dilutions of the peptide from the aggregated state failed to yield reversible aggregation curves, as shown in Figs. 4 and 5. This hysteresis was observed for all of the peptides that associated under these conditions. Rapid dilution of aggregated peptides to one-half of their concentration yielded aggregates that dissociated over a time scale of several hours. *Insets* to Figs. 4 and 5 show the time course of this disaggregation process for D-1-17-OBz and D-1-10-OBz, respectively. The dissociation process could not be fitted to a single exponential decay (Figs. 4 and 5), suggesting that it is not a first order process. Fig. 6 shows the effect of urea on D-1-10-OBz and D-1-17-OBz at constant peptide concentration. Urea disaggregates the peptides and the process is essentially complete at a concentration of 3 M. Fig. 7 shows the effect of NaCl on the aggregation behavior of the 17-residue acid (D-1-17-OH) and ester (D-1-17-OBz). Increasing the salt concentration promotes aggregation of both peptides with D-1-17-OH aggregating only in 3 M NaCl. Fig. 7 demonstrates that D-1-17-OBz is almost completely aggregated by 3 M NaCl, even the minimal detectable concentration of either peptide was associated, with an emission centered at 490 nm. A study of the effect of NaCl concentration on the cmc of D-1-10-OBz establishes a linear relationship for the log-log plot as shown in Fig. 7. Similar results are obtained with CaCl<sub>2</sub>.

**Thermodynamics of Association**—Fig. 8 shows the effect of temperature on the emission spectra of D-1-17-OBz and D-1-10-OBz. Raising the temperature leads to disaggregation of the peptides, *i.e.*  $\Delta H$  is negative for the association process. Van't Hoff plots were constructed for the association of both peptides by determining cmc as a function of temperature (see "Theory"). The results are summarized in the *insets* to Fig. 8. The enthalpies obtained, assuming an aggregation

number of 6, are  $-1.4 \text{ kcal mol}^{-1}$  and  $-3.1 \text{ kcal mol}^{-1}$  for D-1-17-OBz and D-1-10-OBz, respectively.

#### DISCUSSION

The peptides examined in this study consist almost entirely of hydrophobic amino acids. The only polar residue in D-1-10-OBz and D-1-17-OBz is Gln-7. It would, therefore, be anticipated that these peptides may associate in aqueous solution in order to minimize the apolar surface exposed to water. The formation of aggregates in the aqueous phase by these peptides is reminiscent of micelle formation by amphipathic molecules like detergents and phospholipids (31). The absence of oppositely charged groups on the peptide esters eliminates electrostatic interactions as a major source of stabilization for the aggregate. In the case of the peptide acids, repulsion between negatively charged carboxylic acid groups should inhibit aggregation in the absence of suitable counterions. This is, indeed, borne out by the results, which establish that the acids aggregate only at high salt concentrations ( $\sim 3 \text{ M}$ ). From the fluorescence titration data, critical concentrations for "peptide micelle" formation (cmc) can be determined. The decrease in cmc values with increasing chain length and the number of apolar residues further suggests hydrophobic association as the dominant driving force for aggregation. D-1-13-OBz has an anomalously low cmc, the reasons for which are unclear. The cmc of the peptide esters decreases with NaCl concentration. The log-log plot of cmc *versus* NaCl concentration is linear. Such a relationship has been demonstrated for detergent micelles (38), thus strengthening the analogy of peptide aggregates with detergent micelles. The addition of urea to the peptide aggregates results in their dissociation (Fig. 6). Urea has been suggested to denature proteins either by interaction with peptide bonds (39) or by affecting the structure of water and consequently altering hydrophobic effects (40). Either or both of these mechanisms could be active in the disaggregation of highly folded peptides, association of which involves hydrophobic interactions.

Fig. 8 establishes that heat destabilizes the aggregate, *i.e.* the association process is enthalpically favored. Using a treatment similar to that suggested for micelles (see "Theory"), the values of  $\Delta H$  may be estimated. Van't Hoff plots constructed using Equation 4 were linear and yielded values of  $(\bar{m}/\bar{m} - 1) \Delta H = -1.7$  and  $-3.7 \text{ kcal mol}^{-1}$  for D-1-17-OBz and D-1-10-OBz, respectively.  $\bar{m}$  is the average aggregation number. Assuming aggregation numbers of 2 and 10 as the extreme limits,  $\Delta H$  ranges of  $-0.9$  to  $-1.5$  and  $-1.9$  to  $-3.3 \text{ kcal mol}^{-1}$  are obtained for D-1-17-OBz and D-1-10-OBz, respectively. The peptides studied are neutral and by analogy with neutral detergent micelles like Triton X-100 (41), low aggregation numbers are expected. The two peptides are also likely to favor rodlike  $3_{10}$  helical conformations (19, 21, 22). The helical structures have predominantly hydrophobic side chains on the surface, with the exception of the Gln residue. The 3-fold axis of such helical structures coupled with axial translation allow definition of three distinct faces for each helix. One face containing the Gln residue may be designated as polar, while the other two faces are completely nonpolar. Association should then occur by close contact of the nonpolar faces, with the polar face preferentially exposed to the aqueous medium. An attractive arrangement would involve close packing of three or four peptide helices, with a minimum amount of water trapped within the aggregate (Fig. 9). Larger aggregates would require an aqueous channel running through the structure, which would result in an exposure of the interior to water. However, peptide aggregates consisting of more than three or four molecules are not excluded by the available data. It is of interest that hexameric preaggregates of alamethicin

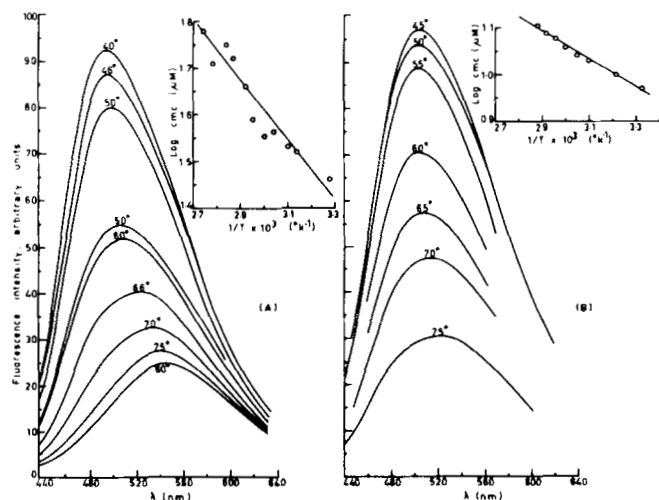


FIG. 8. Effect of temperature on peptide aggregation. Emission spectra of fluorescent alamethicin derivatives, excited at 333 nm, as a function of temperature. *Insets*, van't Hoff plots of log cmc (micromolar) *versus*  $1/T \times 10^3 \text{ (K}^{-1}\text{)}$ . A, D-1-10-OBz (40  $\mu\text{M}$ ); B, D-1-17-OBz (15  $\mu\text{M}$ ).

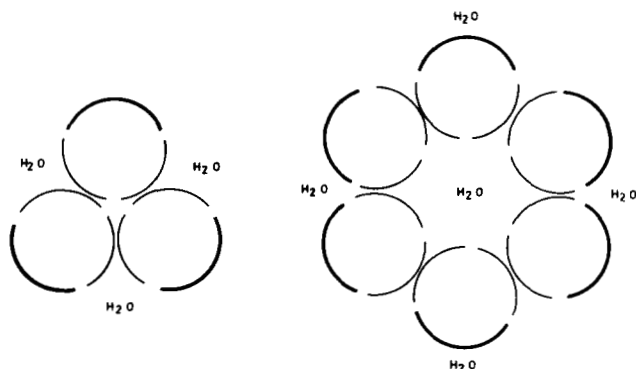


FIG. 9. Model of peptide aggregates. Circles represent cross-sections through aggregates of  $3_{10}$  helical polypeptides. The thick line segment represents the polar face of the helices and the thin line segments the completely apolar faces. Note that in the hexameric aggregate exposure of the apolar faces to external (bulk) water is less than in the trimeric aggregate at the expense of an included (interstitial) aqueous core.

have been postulated at the membrane water interface (23). Such an aggregate would contain a fairly large central aqueous core (Fig. 9). Attempts to determine the size of the aggregates formed by the fluorescent peptides, using Sephadex gel filtration, were unsuccessful. Gel filtration runs in 4 M urea yielded symmetrical peaks corresponding to the monomer. Runs in 2 M NaCl, which should promote aggregation, resulted in precipitation of the peptides on the column. In the absence of salt or urea, broad, poorly characterized bands are obtained. As the gel filtration experiment takes a minimum of 2 h to conduct, extensive dissociation of the aggregates due to dilution can occur. Thus, the broad bands in the elution profile are indicative of monomer-aggregate equilibrium. Aggregation number of alamethicin has been estimated by sedimentation studies to be around 16 at ionic strength 0.2 M (42). The  $\Delta H$  for aggregation becomes less negative with increasing chain length. This is consistent with the results of studies on detergent micelles which establish that  $\Delta H$  for association increases with the length of the apolar segment (43).

Hysteresis has been observed for the aggregation-disaggregation process (Figs. 4 and 5). The rate of disaggregation is nonexponential, indicating that the equilibria involved are complex. Formation of transmembrane channels is probably cooperative, considering the sigmoidal character of the concentration dependence of membrane activity (27, 44). Cooperativity in the membrane phase can be treated by the Ising model in two dimensions. This predicts that for cooperativity parameters less than a critical value, metastable states will exist, leading to hysteresis effects (45). Interesting time-dependent changes in circular dichroism spectra of alamethicin have been reported in organic and aqueous solvent systems (46).

The peptides studied can be ordered in a sequence of decreasing membrane activity. Such sequences constructed for liposomal cation transport and uncoupling of oxidative phosphorylation are found to be identical, indicating that both events have similar structural requirements of peptide chain length and charge. It is thus reasonable to conclude that the same process underlies both events, *viz.* the formation of transmembrane channels. Since membrane-modifying activity increases with chain length and is attenuated by the presence of a negative charge in the acids, it appears that peptide aggregation may be the decisive step in the formation of functional channels. Table I shows that for the peptide esters, membrane-modifying activity correlates well with the ease of aggregation, as reflected by the cmc values. It may be noted that the rate of formation of transmembrane channels is

dependent on two factors, the formation of aqueous phase aggregates and their insertion into the membrane. At low concentrations, the lower the cmc, the greater the amount of aggregated species likely to be present. The correlation demonstrated in Table I between membrane-modifying activity and ease of aggregation indicates that the concentration of aggregated species dominates the rate of formation of transmembrane channels.

Aggregation of the peptide acids is not observed up to 50  $\mu\text{M}$  in salt-free aqueous media, but membrane activity of D-1-17-OH is detected at much lower concentrations (Table I). However, acids do aggregate at high ionic strength (Fig. 7). Estimates of the concentration of cations in the Stern layer of sodium dodecyl sulfate micelles range from 1 to 3 M (47) and are likely to be in the same range at membrane surfaces also. Furthermore, experimental protocol requires injection of aliquots of concentrated peptide solutions to the test system. The rates of disaggregation are very much slower than the insertion of peptide aggregates into the membrane (Figs. 1, 4, and 5). Thus, the "memory effect" in peptide aggregates may also be of relevance in explaining the observation of membrane-modifying activity in D-1-17-OH at concentrations below its cmc in salt-free solution.

While ease of aggregation correlates well with functional activity, aggregation itself is not a sufficient criterion for activity. For example, D-1-10-OBz aggregates at 30  $\mu\text{M}$  but is inactive at that concentration. This is not surprising since a minimum chain length would be necessary for the formation of transmembrane channels. Earlier studies have suggested that a length of approximately 13 residues is the minimum required for the detection of membrane activity (27, 28).

The results described in this report establish that membrane channel-forming hydrophobic peptides aggregate in aqueous solution and that membrane-modifying activity correlates well with the ease of aggregation. Peptide association is favored in media of high ionic strength. This is particularly relevant since peptide acids aggregate only at high ionic strength and the ionic concentrations in the Stern layer of micelles and surfaces of membranes are likely to be high. The results of the present study favor a model for preformed aggregate into the lipid bilayer (23).

*Acknowledgment*—We wish to thank Professor C. K. R. Kurup for providing facilities for the uncoupling assays.

#### REFERENCES

- Mueller, P., and Rudin, D. O. (1968) *Nature* **217**, 713-719
- Pandey, R. C., Cook, J. C., Jr., and Rinehart, K. L., Jr. (1977) *J. Am. Chem. Soc.* **99**, 8469-8483
- Marshall, G. R., and Bosshard, H. E. (1972) *Circ. Res.* **30**, Suppl. II, 143-150
- Jung, G., König, W. A., Liebfritz, D., Ooka, T., Janko, K., and Boheim, G. (1976) *Biochim. Biophys. Acta* **433**, 164-181
- Boheim, G., Janko, K., Liebfritz, D., Ooka, T., König, W. A., and Jung, G. (1976) *Biochim. Biophys. Acta* **433**, 182-199
- Boheim, G., Irmscher, G., and Jung, J. (1978) *Biochim. Biophys. Acta* **507**, 485-506
- Jones, L. R., Besch, H. R., Jr., and Watanabe, A. M. (1977) *J. Biol. Chem.* **252**, 3315-3323
- Besch, H. R., Jr., Jones, L. R., Fleming, J. W., and Watanabe, A. M. (1977) *J. Biol. Chem.* **252**, 7905-7908
- Irmscher, G., and Jung, G. (1977) *Eur. J. Biochem.* **80**, 165-174
- Bessler, W. G., Ottenbreit, B., Irmscher, G. and Jung, G. (1979) *Biochem. Biophys. Res. Commun.* **87**, 99-105
- Lau, A. L. Y., and Chan, S. I. (1974) *Biochemistry* **13**, 4942-4948
- Shamala, N., Nagaraj, R., and Balaram, P. (1978) *J. Chem. Soc. Chem. Commun.* 996-997
- Prasad, B. V. V., Shamala, N., Nagaraj, R., Chandrasekaran, R., and Balaram, P. (1979) *Biopolymers* **18**, 1635-1646



14. Prasad, B. V. V., Shamala, N., Nagaraj, R., and Balaram, P. (1980) *Acta Crystallogr.* **B36**, 107-110
15. Venkatachalapathi, Y. V., Nair, C. M. K., Vijayan, M., and Balaram, P. (1981) *Biopolymers* **20**, 1123-1136
16. Venkatachalapathi, Y. V., and Balaram, P. (1981) *Biopolymers* **20**, 1137-1145
17. Nagaraj, R., Shamala, N., and Balaram, P. (1979) *J. Am. Chem. Soc.* **101**, 16-20
18. Rao, Ch.P., Nagaraj, R., Rao, C. N. R., and Balaram, P. (1980) *Biochemistry* **19**, 425-431
19. Nagaraj, R., and Balaram, P. (1981) *Biochemistry* **20**, 2828-2835
20. Smith, G. D., Pletnev, V. Z., Duax, W. L., Balasubramanian, T. M., Bosshard, H. E., Czerwinski, E. W., Kendrick, N. E., Mathews, F. S., and Marshall, G. R. (1981) *J. Am. Chem. Soc.* **103**, 1493-1501
21. Iqbal, M., and Balaram, P. (1981) *J. Am. Chem. Soc.* **103**, 5548-5552
22. Iqbal, M., and Balaram, P. (1981) *Biochemistry* **20**, 4866-4871
23. Boheim, G., and Kolb, H. A. (1978) *J. Membr. Biol.* **38**, 99-150
24. Baumann, G., and Mueller, P. (1974) *J. Supramol. Struct.* **2**, 538-556
25. Edmonds, D. T. (1979) *Chem. Phys. Lett.* **65**, 429-433
26. Fringeli, U. P. (1980) *J. Membr. Biol.* **54**, 203-212
27. Nagaraj, R., Mathew, M. K., and Balaram, P. (1980) *FEBS Lett.* **121**, 365-368
28. Mathew, M. K., Nagaraj, R., and Balaram, P. (1981) *Biochem. Biophys. Res. Commun.* **98**, 548-555
29. Nagaraj, R., and Balaram, P. (1979) *Biochem. Biophys. Res. Commun.* **89**, 1041-1049
30. Fisher, L. R., and Oakenfull, D. G. (1977) *Chem. Soc. Rev.* **6**, 25-42
31. Tanford, C. (1973) *The Hydrophobic Effect: Formation of Micelles and Biological Membranes*, Wiley, New York
32. Nagaraj, R., and Balaram, P. (1981) *Tetrahedron* **37**, 1263-1270
33. Brunner, J., Skrabal, P., and Hauser, H. (1976) *Biochim. Biophys. Acta* **455**, 322-331
34. Johnson, D., and Lardy, H. A. (1967) *Methods Enzymol.* **10**, 94-96
35. Gornall, A. G., Bardawill, D. J., and David, M. M. (1949) *J. Biol. Chem.* **177**, 751-766
36. Caswell, A. H., and Hutchison, J. D. (1971) *Biochem. Biophys. Res. Commun.* **43**, 625-630
37. Takaishi, Y., Terada, H., and Fujita, T. (1980) *Experientia* **36**, 550-552
38. Shick, M. J. (1964) *J. Phys. Chem.* **68**, 3585-3592
39. Roseman, M., and Jencks, W. P. (1975) *J. Am. Chem. Soc.* **97**, 631-640
40. Franks, F. (1975) in *Water: A Comprehensive Treatise* (Franks, F., ed) Vol. 4, pp. 1-94, Plenum Press, New York
41. Fendler, E. J., and Fendler, J. H. (1975) *Catalysis in Micellar and Macromolecular Systems*, Academic Press, New York
42. McMullen, A. I., and Stirrup, J. A. (1971) *Biochim. Biophys. Acta* **241**, 807-814
43. Corkill, J. M., Goodman, J. F., Robson, P., and Tate, J. R. (1966) *Trans. Faraday Soc.* **62**, 987-993
44. Schindler, H., and Rosenbusch, J. P. (1981) *Proc. Natl. Acad. Sci. U. S. A.* **78**, 2302-2306
45. Stankowski, S., and Gruenwald, B. (1980) *Biophys. Chem.* **12**, 167-176
46. Jung, G., Dubischar, N., and Leibfritz, D. (1975) *Eur. J. Biochem.* **54**, 395-409
47. Mukerjee, P. (1962) *J. Phys. Chem.* **66**, 943-945